

Observation of an inter-sublattice exchange magnon in CoCr_2O_4 and analysis of magnetic ordering

D. Kamenskyi,¹ H. Engelkamp,² T. Fischer,¹ M. Uhlarz,¹ J. Wosnitzer,¹ B. P. Gorshunov,^{3,4,5} G. A. Komandin,³ A. S. Prokhorov,^{3,4} M. Dressel,⁵ A. A. Bush,⁶ V. I. Torgashev,⁷ and A. V. Pronin^{1,*}

¹*Dresden High Magnetic Field Laboratory (HLD),*

Helmholtz-Zentrum Dresden-Rossendorf, 01314 Dresden, Germany

²*High Field Magnet Laboratory, Institute for Molecules and Materials, Radboud University Nijmegen, 6525 ED Nijmegen, The Netherlands*

³*A. M. Prokhorov Institute of General Physics, Russian Academy of Sciences, 119991 Moscow, Russia*

⁴*Moscow Institute of Physics and Technology (State University), 141700 Dolgoprudny, Moscow Region, Russia*

⁵*1. Physikalisches Institut, Universität Stuttgart, Pfaffenwaldring 57, 70550 Stuttgart, Germany*

⁶*Moscow State Institute of Radio-Engineering, Electronics,*

and Automation (Technical University), 117464 Moscow, Russia

⁷*Faculty of Physics, Southern Federal University, 344090 Rostov-on-Don, Russia*

(Dated: May 24, 2022)

We report on an investigation of optical properties of multiferroic CoCr_2O_4 at terahertz frequencies in magnetic fields up to 30 T. Below the ferrimagnetic transition (94 K), the terahertz response of CoCr_2O_4 is dominated by a magnon mode, which shows a steep magnetic-field dependence. We ascribe this mode to an exchange resonance between two magnetic sublattices with different g -factors. In the framework of a simple two-sublattice model (the sublattices are formed by Co^{2+} and Cr^{3+} ions), we find the inter-sublattice coupling constant, $\lambda = -(18 \pm 1)$ K, and trace the magnetization for each sublattice as a function of field. We show that the Curie temperature of the Cr^{3+} sublattice, $\Theta_2 = (49 \pm 2)$ K, coincides with the temperature range, where anomalies of the dielectric and magnetic properties of CoCr_2O_4 have been reported in literature.

PACS numbers: 75.85.+t, 76.50.+g

CoCr_2O_4 is a ferrimagnetic spinel compound with a complex network of competing magnetic interactions.^{1,2} Both, Co^{2+} (A sites of the spinel structure) and Cr^{3+} ions (B1 and B2 sites), are magnetic. Below the Curie temperature, $T_C = 94$ K, the system exhibits a long-range ferrimagnetic order.¹ At $T_S = 26$ K, a structural transition occurs. Below this temperature, an incommensurate conical (i.e. uniform plus transverse spiral) magnetic structure sets in. At $T_{\text{lock-in}} = 15$ K, the magnetic structure becomes commensurate – the period of the spin spiral “locks” to the lattice parameter.²

The spiral order most likely survives above T_S , but on short ranges only.^{1,2} At $T_{\text{kink}} = 50$ K, anomalies in dielectric and magnetic properties of CoCr_2O_4 have been reported^{3,4} and tentatively attributed to the formation of this incommensurate short-range spiral magnetic order.⁴

In 2006, Yamasaki *et al.* have discovered the structural transition at $T_S = 26$ K to be accompanied by the emergence of a spontaneous electric polarization, which direction can be reversed by applying a magnetic field.⁵ As multiferroics are appealing because of basic physical interest as well as their potential technological applications,⁶ the reported multiferroicity of CoCr_2O_4 has triggered a number of experimental studies of the compound.^{4,7–10} To date, there is, however, no optical data reported at terahertz frequencies. This is the frequency region where *e.g.* electromagnons have been observed in some other multiferroic systems.^{11,12}

Here, we report on an optical study of CoCr_2O_4 at terahertz (or far-infrared) frequencies in magnetic fields up

to 30 T. We do not find any evidence for electromagnons. However, below T_C , we observe a resonance mode, which is highly sensitive to external magnetic field. We ascribe this mode to a ferrimagnetic inter-sublattice exchange resonance, originally considered theoretically by Kaplan and Kittel.¹³ Applying this model to CoCr_2O_4 allows us to separate the contributions of the Co^{2+} and Cr^{3+} sublattices to the total magnetization, to extract the magnetization for each sublattice as a function of field, and to find the inter-sublattice coupling constant. Furthermore, we show that the Curie temperature of the Cr^{3+} sublattice coincides with $T_{\text{kink}} = 50$ K. Thus, the onset of the short-range spiral component must be related to the ordering in the Cr^{3+} sublattice.

The investigated CoCr_2O_4 samples have been synthesized from Co_3O_4 and Cr_2O_3 powders. CoCr_2O_4 powder has been pressed into pellets of 10 mm in diameter and 1 mm in thickness. X-ray diffraction measurements prove the cubic symmetry (space group $Fd\bar{3}m$) with no indication of spurious phases. The lattice constant, $a = 8.328(2)$ Å, is in good agreement with published results.^{14,15} More details on sample preparation, characterization, and thermodynamic properties of CoCr_2O_4 are given in our recent works.^{3,16}

The optical measurements have been made in transmission mode, using two different setups. The first setup was a spectrometer equipped with backward-wave oscillators (BWOs) as sources of coherent and frequency-tunable radiation.^{17,18} The measurements were done at (sub)terahertz frequencies ($\nu = \omega/2\pi = 8.5 \div 41$ cm⁻¹ =

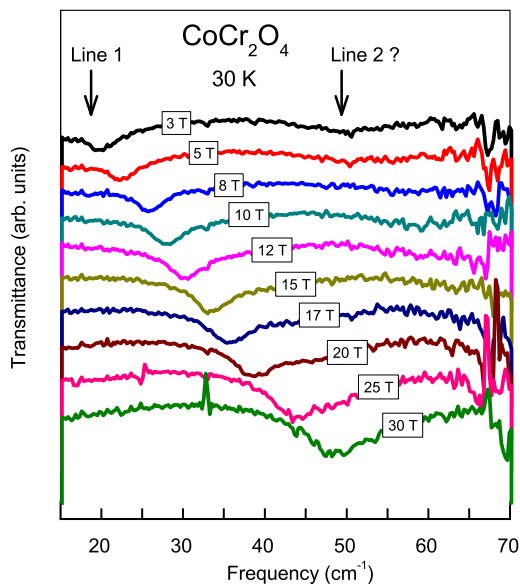


FIG. 1: (Color online) Examples of raw far-infrared transmittance spectra of CoCr_2O_4 in Faraday geometry. The absorption line, marked as “Line 1”, is discussed in the course of the article. At the higher-frequency end of the spectra, there is an indication of another, very broad, line (“Line 2 ?”).

$250 \div 1230 \text{ GHz} = 1 \div 5 \text{ meV}$) and at temperatures between 4 and 300 K. The radiation was linearly polarized. The absolute values of optical transmission (normalized to the empty-channel measurements) were obtained in essentially the same way as described, e.g., in Ref. 19.

A commercial split-coil magnet, embedded into an optical cryostat, was utilized for measurements in magnetic fields up to 8 T. In these measurements, we used three different geometries: $\mathbf{k} \perp \mathbf{H} \parallel \hat{\mathbf{h}}$, $\mathbf{k} \perp \mathbf{H} \perp \hat{\mathbf{h}}$, and $\mathbf{k} \parallel \mathbf{H} \perp \hat{\mathbf{h}}$ (here \mathbf{H} is the external static magnetic field; \mathbf{k} and $\hat{\mathbf{h}}$ are the wave vector and the magnetic component of the probing electromagnetic radiation, respectively).

In the first geometry ($\mathbf{k} \perp \mathbf{H} \parallel \hat{\mathbf{h}}$), where electromagnons, if they exist, could be excited, we did not observe any resonance absorption lines. Furthermore, these spectra show no detectable changes induced by applying magnetic fields up to 8 T.

In the two other geometries (where $\mathbf{H} \perp \hat{\mathbf{h}}$), we observed absorption lines. We did not detect any differences between the results for these two geometries, although the data obtained for $\mathbf{k} \parallel \mathbf{H}$ (Faraday geometry) are somewhat less noisy due to peculiarities of the split-coil magnet design. Thus, in the following we discuss the BWO data collected in the Faraday geometry.

The second optical setup was a commercial Fourier-transform infrared (FTIR) spectrometer (Bruker IFS113v) combined with a continuous-field 33-Tesla Bitter magnet, at the High Field Magnet Laboratory in Nijmegen.²⁰ The measurements were performed in the Faraday geometry ($\mathbf{k} \parallel \mathbf{H} \perp \hat{\mathbf{h}}$) at 4 and 30 K. A mercury lamp was used as a radiation source. The far-infrared

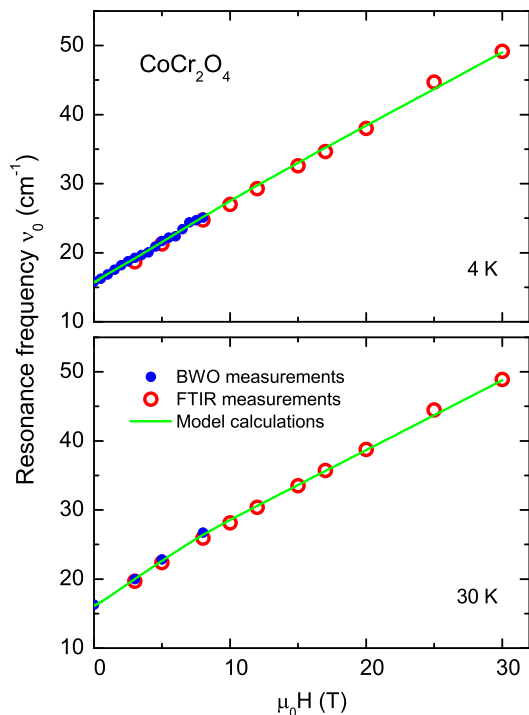


FIG. 2: (Color online) Field dependence of the magnon frequency for 4 and 30 K. Symbols are the experimental data, lines represent the results of simultaneous fits of the optical data with Eq. 3 and of magnetization data from Ref. 3 with Eqs. 1 and 2. Note that the onset of the vertical scales is at 10 cm^{-1} .

radiation was detected using a custom-made silicon bolometer operating at 1.4 K. For both temperatures, the FTIR spectra were measured in 0, 3, 5, 8, 10, 12, 15, 17, 20, 25, and 30 T. The optical data were collected between 15 and 70 cm^{-1} ($450 \div 2100 \text{ GHz}$, $1.9 \div 8.7 \text{ meV}$), using a $200\text{-}\mu\text{m}$ mylar beamsplitter and a scanning velocity of 50 kHz. At each field, at least 100 scans were averaged.

In the transmission spectra, obtained by use of both setups, we reliably observed an intensive absorption line, which is highly sensitive to the applied magnetic field and temperature (“Line 1” in Fig. 1). At the higher-frequency end of the FTIR spectra, we possibly observe another, broad and weak, absorption line (“Line 2 ?” in Fig. 1). The position of this line shifts to higher frequencies (and thus out of the measurement-frequency window) in applied magnetic field. We tentatively attribute this line to an antiferromagnetic resonance within the Cr^{2+} sublattice. Hereafter, we solely discuss the “Line 1”.

The field dependence of the frequency of “Line 1”, ν_0 , is shown in Fig. 2. The resonance frequency is basically proportional to the applied static field with a zero-field gap. At 4 K, the gap is 15.8 cm^{-1} (475 GHz , 1.97 meV), and at 30 K, it is 16.3 cm^{-1} (489 GHz , 2.02 meV). At low fields [$\mu_0 H \lesssim 10 \text{ T}$], the dimensionless slopes of the $\nu_0(H)$

curves, $h\nu_0/\mu_B\mu_0H$, reach 2.5 (at 4 K) and 2.8 (at 30 K). Let us note, that the typical slopes of the $\nu_0(H)$ curves for ferromagnetic resonances in the Co^{2+} - or Cr^{3+} -based compounds are determined by the gyromagnetic ratios of the Co^{2+} and Cr^{3+} ions and amount to 2.2 and 1.95, respectively.²¹

Resonance modes in ferrimagnetic substances have originally been considered theoretically by Kaplan and Kittel.¹³ For a system with two magnetic sublattices, they predicted the existence of two magnetic-resonance lines. The first of them is associated with the conventional spin precession. In CoCr_2O_4 , such mode has been observed by electron-spin-resonance studies at frequencies below 100 GHz in fields up to 10 T.^{22,23} The second mode, the inter-sublattice exchange resonance, is supposed to have a large zero-field gap defined by the exchange interaction between the sublattices, to harden in an applied magnetic field, and to have a steep field dependence.²⁴ Our observed mode demonstrates this very behavior (Fig. 2). Thus, it is reasonable to associate it with the Kaplan-Kittel inter-sublattice exchange resonance.

In the following, we show that using a simple two-sublattice Kaplan-Kittel model, we can consistently describe our data on the magnon frequency and our earlier data on magnetization (Ref. 3). From this description, we obtain the magnetic moments of the sublattices and the inter-sublattice exchange constant.

In our model, we consider two effective magnetic sublattices. Coupling within the first sublattice is provided by exchange interactions between Co^{2+} and Cr^{3+} ions, J_{AB} . At $\Theta_1 = T_C = 94$ K, this sublattice orders. Important is that only non-collinearly ordered spins of the Co^{2+} ions contribute to the magnetic moment, while the spins of the Cr^{3+} ions do not. This is because of geometrical frustration of the interaction between the Cr^{3+} ions, J_{BB} .² Thus, one can consider the first sublattice to be formed by Co^{2+} ions only.

When temperature decreases further, the Cr^{3+} spins start to contribute (negatively) to the net magnetization. Thus, as the second sublattice, one can consider the sublattice formed by Cr^{3+} ions. Let us note, that because of geometrical frustration, the effective coupling within the Cr^{3+} sublattice is significantly smaller than J_{BB} . The Curie temperature of this sublattice, Θ_2 , is somewhere below 94 K. This temperature will be one of our fit parameters (we take Θ_2 to be field independent).

For a two-sublattice ferrimagnet, the net (measurable) magnetization is the sum of the magnetizations of the sublattices, $M(T, H) = M_1(T, H) + M_2(T, H)$. M_1 and M_2 have opposite signs; the inter-sublattice exchange constant λ is negative. Within the molecular-field approximation, the reduced magnetization of each sublattice, $y_i \equiv M_i/M_i^0$ [here and thereafter $i = \{1, 2\} \equiv \{\text{Co}^{2+}, \text{Cr}^{3+}\}$ and M_i^0 is the zero-temperature magnetization of the i -th sublattice], is given by the Brillouin

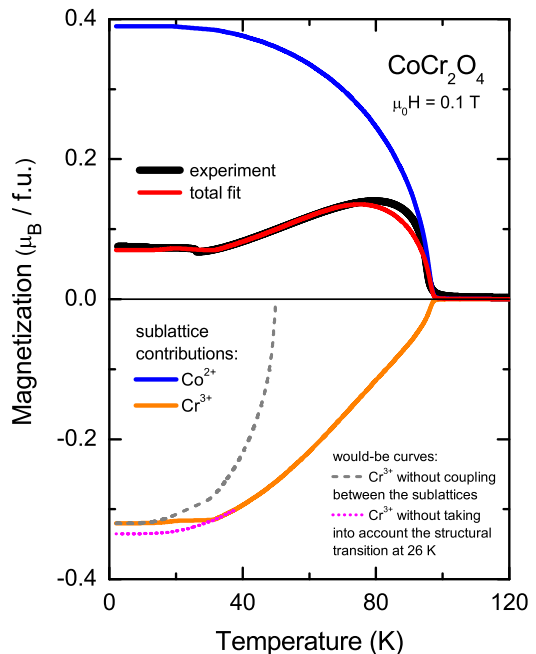


FIG. 3: (Color online) Example of a fit by use of Eqs. 1 and 2 to the magnetization data obtained at 0.1 T [simultaneously, the magnon-frequency data were fitted with the same set of free parameters, see Fig. 2]. Contributions of the Co^{2+} and Cr^{3+} sublattices are shown with opposite signs. The contribution of the Cr^{3+} sublattice diminishes at T_C , rather than at $\Theta_2 = 49$ K, because of the coupling between the sublattices.

function:^{25,26}

$$y_i = B_{S_i}(x_i) \equiv \frac{2S_i + 1}{2S_i} \coth \frac{2S_i + 1}{2S_i} x_i - \frac{1}{2S_i} \coth \frac{x_i}{2S_i}, \quad (1)$$

where S_i is the spin magnetic moment for ions of the i -th sublattice and x_i is defined as:

$$x_i = \frac{\mu_B}{k_B T} \left[\frac{3S_i}{S_i + 1} \left(\frac{k_B \Theta_i M_i}{\mu_B M_i^0} + \frac{k_B \lambda M_j}{\mu_B M_i^0} \right) + H M_i^0 \right], \quad (2)$$

$i \neq j.$

In our case, Co^{2+} and Cr^{3+} ions have equal spin moments, $S_1 = S_2 = 3/2$.

For the resonance frequency ν_0 , we use a modified Kaplan-Kittel equation:^{10,13}

$$\left(\frac{h\nu_0}{\mu_B g_1} + \frac{k_B}{\mu_B} \lambda M_2 + H \right) \times \left(\frac{h\nu_0}{\mu_B g_2} - \frac{k_B}{\mu_B} \lambda M_1 + H \right) + \left(\frac{k_B}{\mu_B} \lambda \right)^2 M_1 M_2 = 0, \quad (3)$$

where $g_1 = 2.2$ and $g_2 = 1.95$ are the gyromagnetic ratios for the Co^{2+} and Cr^{3+} ions, respectively.²¹ In Eqs. 2 and 3, magnetization is in dimensionless units. In our model, we neglect anisotropy, as our measurements have been performed on powder samples.²⁷

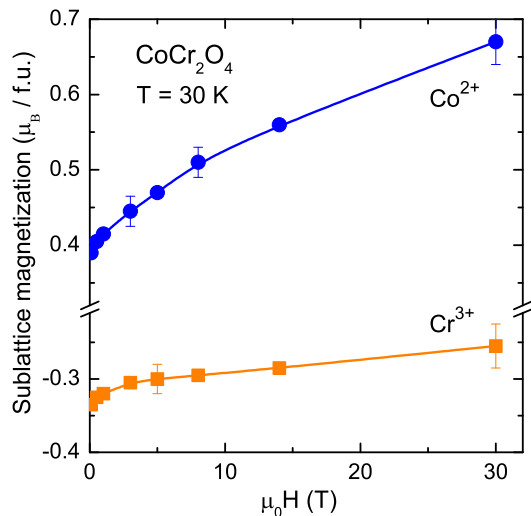


FIG. 4: (Color online) Magnetization of the Co^{2+} and Cr^{3+} sublattices in CoCr_2O_4 , as obtained from the model fits with Eqs. 1 – 3. The lowest-field points are at 0.1, 0.5, and 1 T.

Unlike in collinear ferrimagnetics, in CoCr_2O_4 the vector of the magnetization of each sublattice in an external magnetic field can change not only its orientation, but also its size. In our calculations, we take this into account. The corresponding increase in M_1^0 and M_2^0 is supposed to persist until the spin-only values for Co^{2+} and Cr^{3+} ions of $3 \mu_B/\text{ion}$ are reached. Recent experiments in pulsed magnetic fields have shown that even in fields of up to 60 T, there are no signs of saturation in the magnetization.²⁸

Using Eqs. 1 – 3, we simultaneously fit the magnetization data, obtained in Ref. 3, and our results for the resonance frequency.²⁹ Results of these fits are shown in Figs. 2 and 3 together with experimental data. We find that the best description of all our experimental data can be reached with $\lambda = -(18 \pm 1)$ K and $\Theta_2 = (49 \pm 2)$ K.

The value found for the ordering temperature of the Cr^{3+} sublattice, Θ_2 , coincides with T_{kink} – the temperature, which is possibly related to the formation of the incommensurate short-range spiral magnetic order.⁴ Our findings show that this short-range order appears to be due to the involvement of the Cr^{3+} ions. The relatively large value of the coupling constant, $\lambda = -18$ K, may explain why the T_{kink} -related features appear to be broad.^{2,4}

Figure 4 shows the magnetic-field dependence of the calculated sublattice magnetizations. We show here the results obtained at $T = 30$ K, i.e. just above the structural transition. As it can be seen from Fig. 3, the lower-temperature results differ only marginally from the shown in Fig. 4. We have found that within our model, the observed behavior of the experimental data at T_S can be best described by a slight decrease in the absolute value of M_{Cr} at T_S (the g -factors of the Co^{2+} and Cr^{3+} ions are presumed to be independent of temperature).

The contribution of each sublattice to the total magnetic moment in zero field can be estimated from Fig. 4. We find $M_{Co}(0 \text{ T}) = 0.4 \mu_B/\text{f.u.}$ and $M_{Cr}(0 \text{ T}) = -0.33 \mu_B/\text{f.u.}$ We note, that although in fields smaller than the coercive force (0.3 T, Ref. 3) the M_i values are influenced by the magnetizing/demagnetizing processes, this influence hardly affects the above result [in Fig. 4, only the lowest-field point (0.1 T) is below the coercive-force value, the next points are at 0.5 and 1 T].

The proposed model gives a natural explanation for the steep slope of the $\nu_0(H)$ curves [Fig. 2]. As can be seen from Eq. 3, this is due to the increase of M_i as a function of field. Similarly, the temperature evolution of $\nu_0(H)$ is explained as being due to the temperature evolution of the $M_i(H)$ curves.

Summarizing, the far-infrared optical response of CoCr_2O_4 below the Curie temperature, $T_C = 94$ K, is dominated by a magnon mode. Ascribing the magnon to an inter-sublattice exchange resonance (the sublattices are formed by the Co^{2+} and Cr^{3+} ions) and applying a modified Kaplan-Kittel model of two interacting sublattices allows us to consistently describe our experimental data on the magnon frequency and earlier magnetization measurements, to obtain the magnetization for each of the sublattices, and to find the inter-sublattice exchange constant, $\lambda = -18$ K. The Curie temperature of the Cr^{3+} sublattice is found to coincide with the temperature, where the incommensurate short-range spiral magnetic order is believed to set in, $T_{\text{kink}} = 50$ K.

We thank M. D. Kuz'min for useful discussions and Papori Gogoi for assistance in measurements. Parts of this work were supported by EuroMagNET II (EU contract No. 228043), by the Russian Foundation for Basic Research (Grant No. 12-02-00151) and by the Ministry of Education and Science of the Russian Federation (contract No. 14.A18.21.0740).

* Electronic address: a.pronin@hzdr.de

¹ N. Menyuk, K. Dwight, and A. Wold, *J. Phys. (Paris)* **25**, 528 (1964).

² K. Tomiyasu, J. Fukunaga, and H. Suzuki, *Phys. Rev. B* **70**, 214434 (2004).

³ A. V. Pronin, M. Uhlarz, R. Beyer, T. Fischer, J. Wosnitza, B. P. Gorshunov, G. A. Komandin, A. S. Prokhorov, M. Dressel, A. A. Bush, and V. I. Torgashev, *Phys. Rev. B*

85, 012101 (2012).

⁴ G. Lawes, B. Melot, K. Page, C. Ederer, M. A. Hayward, Th. Proffen, and R. Seshadri, *Phys. Rev. B* **74**, 024413 (2006).

⁵ Y. Yamasaki, S. Miyasaka, Y. Kaneko, J.-P. He, T. Arima, and Y. Tokura, *Phys. Rev. Lett.* **96**, 207204 (2006).

⁶ T. Kimura, T. Goto, H. Shintan, K. Ishizaka, T. Arima, and Y. Tokura, *Nature* **426**, 55 (2003).

- ⁷ Y. J. Choi, J. Okamoto, D. J. Huang, K. S. Chao, H. J. Lin, C. T. Chen, M. van Veenendaal, T. A. Kaplan, and S.-W. Cheong, *Phys. Rev. Lett.* **102**, 067601 (2009).
- ⁸ N. Mufti, A. A. Nugroho, G. R. Blake, and T. T. M. Palstra, *J. Phys.: Condens. Matter* **22**, 075902 (2010).
- ⁹ L. J. Chang, D. J. Huang, W.-H. Li, S.-W. Cheong, W. Ratcliff, and J. W. Lynn, *J. Phys.: Condens. Matter* **21**, 456008 (2010).
- ¹⁰ V. I. Torgashev, A. S. Prokhorov, G. A. Komandin, E. S. Zhukova, V. B. Anzin, V. M. Talanov, L. M. Rabkin, A. A. Bush, M. Dressel, and B. P. Gorshunov, *Phys. Solid State* **54**, 350 (2012).
- ¹¹ A. Pimenov, A. A. Mukhin, V. Y. Ivanov, V. D. Travkin, A. M. Balbashov, and A. Loidl, *Nat. Phys.* **2**, 97 (2006).
- ¹² A. B. Sushkov, R. V. Aguilar, S.-W. Cheong, and H. D. Drew, *Phys. Rev. Lett.* **98**, 027202 (2007).
- ¹³ J. Kaplan and C. Kittel, *J. Chem. Phys.* **21**, 760 (1953).
- ¹⁴ B. Mansour, N. Baffier, and M. Huber, *C. R. Hebd. Seances Acad. Sci., Ser. C* **277**, 867 (1973).
- ¹⁵ P. G. Casado and I. Rasines, *Polyhedron* **5**, 787 (1986).
- ¹⁶ M. Uhlarz, A. V. Pronin, J. Wosnitza, A. S. Prokhorov, and A. A. Bush, *Phys. Chem. Minerals* **40**, 203 (2013).
- ¹⁷ G. V. Kozlov and A. A. Volkov, in *Millimeter and Submillimeter Wave Spectroscopy of Solids*, edited by G. Grüner (Springer, Berlin, 1998), p. 51.
- ¹⁸ B. Gorshunov, A. Volkov, I. Spektor, A. Prokhorov, A. Mukhin, M. Dressel, S. Uchida, and A. Loidl, *Int. J. Infrared Millim. Waves* **26**, 1217 (2005).
- ¹⁹ A. Mukhin, B. Gorshunov, M. Dressel, C. Sangregorio, and D. Gatteschi, *Phys. Rev. B* **63**, 214411 (2001).
- ²⁰ S. A. J. Wieggers, P. C. M. Christianen, H. Engelkamp, A. den Ouden, J. A. A. J. Perenboom, U. Zeitler, and J. C. Maan, *J. Low Temp. Phys.* **159**, 389 (2010).
- ²¹ S. A. Altshuler and B. M. Kozyrev, *Electron Paramagnetic Resonance in Compounds of Transition Elements* (Wiley, New York, 1974).
- ²² J. J. Stickler and H. J. Zeiger, *J. Appl. Phys.* **39**, 1021 (1968).
- ²³ S. Funahashi, K. Siratori, and Y. Tomono, *J. Phys. Soc. Jpn.* **29**, 1179 (1970).
- ²⁴ T. A. Kaplan, *Phys. Rev.* **109**, 782 (1958).
- ²⁵ S. V. Vonsovsky, *Magnetism* (Wiley, New York, 1974).
- ²⁶ M. D. Kuz'min and A. M. Tishin, *Cryogenics* **32**, 545 (1992).
- ²⁷ In practice, this approximation would also be valid for single crystals, as the magnitude of the anisotropy field in CoCr_2O_4 is below 0.1 T [Ref. 23], i.e. significantly smaller than all terms in Eqs. 2 and 3 for external fields above 0.1 T.
- ²⁸ V. Tsurkan, S. Zherlitsyn, S. Yasin, V. Felea, Y. Skourski, J. Deisenhofer, H.-A. Krug von Nidda, J. Wosnitza, and A. Loidl, *Phys. Rev. Lett.* **110**, 115502 (2013).
- ²⁹ Since no experimental data on the temperature dependence of the magnetization at 30 T are available, we used a linear extrapolation of the magnetization in accordance with the $M(H)$ measurements of Ref. 28.